Phenothiazine−Pyrene Dyads: Photoinduced Charge Separation and Structural Relaxation in the CT State

Nursel Acar,[†] Jana Kurzawa,[†] Norbert Fritz,[†] André Stockmann,[†] Ciprian Roman,[†] Siegfried Schneider,*[,†] and Timothy Clark[‡]

Institut für Physikalische und Theoretische Chemie, Friedrich-Alexander-Universität Erlangen, Nürnberg, D-91058 Erlangen, Germany, and Computer-Chemie-Centrum, Friedrich-Alexander-Universität Erlangen-Nürnberg, D-91052 Erlangen, Germany

Received: August 1, 2003; In Final Form: September 3, 2003

Electron donor−acceptor systems with phenothiazine linked directly to pyrene exhibit a dual emission in moderately and very polar solvents. Steady state and time-resolved fluorescence spectroscopy provide evidence that the "blue" and "red" emission bands originate from different species. Fluorescence excitation spectra show a similar appearance when the emission is monitored either in the red or blue spectral range, but they are slightly shifted against each other. This suggests that different isomers exist with a distinctly different photophysical behavior. Semiempirical (AM1/CI) molecular orbital calculations with a continuum solvent treatment have been used to establish the geometry of the two nearly isoenergetic stereoisomers and to calculate the properties of their excited Franck−Condon states. Geometry optimization of various excited states provides evidence for different internal relaxation coordinates for the phenothiazine-localized S_1 state and the charge transfer state S_6, on one hand, and the pyrene-localized S_2 (S_3) state, on the other hand. The relaxed geometries in the excited states of both isomers represent mirror images with identical properties. The different photophysical behavior of the two isomers is most likely caused by the different potential energy curves, or more precisely speaking, by different location and/or heights of the barrier along the reaction coordinates from the locally excited to the geometry-relaxed CT states.

1. Introduction

During the past decade, numerous investigations have been aimed at a better understanding of (photoinduced) intramolecular electron transfer[1−10] and especially at the correlation between the rate of this process, k_{et}, and the overall geometry of the donor−bridge−acceptor (D−B−A) system. More recently, special attention has been given to the fact that conformational parameters such as rotation around a single or double bond connecting the bridging element or folding of a semiflexible bridging element like a piperidyl ring, which alter both distance and relative orientation of donor and acceptor, can be decisive factors for the photophysical properties of charge transfer states.[11−13] Because of the difference in Gibbs energy required for charge separation and recombination, the two processes can occur with greatly different rates in different conformers.[14] They are, in addition, sensitively dependent on solvent polarity, whenever the distance for charge separation varies significantly between different conformers.

An interesting constituent element, which can lead to pronounced conformational heterogeneity in the electronic ground state, is phenothiazine, because the N substituent (bridging element) can adopt a quasiaxial or quasiequatorial position.[15] Moreover, it is well established that the hybridization of the nitrogen changes upon electronic excitation. In the case of complete electron withdrawal (oxidation) the nitrogen can even adopt a planar binding pattern (sp^2 hybridization).[16]

In three previous publications, we have reported the results of transient absorption,[17] time-resolved fluorescence,[18] and Raman experiments[19] performed with D−B−A systems comprising phenothiazine as the donor, pyrene as the acceptor, and a phenyl ring as the bridging elements. The results of these experiments provided evidence that photoinduced electron transfer occurs with rate constants on the order of $k_{et} \approx 10^{11}$ s^{-1} in these compounds. The magnitude of the rate implies that fluorescence from locally excited (LE) states, which act as precursors of the charge transfer (CT) states, should be heavily quenched. Nevertheless, we observed a fairly strong fluorescence in the spectral region in which fluorescence originating from the LE states of pyrene and phenothiazine is expected. We therefore showed that the compounds investigated exist in solution in two forms: (i) as a majority species, whose conformation is the same as that found in crystalline material by X-ray analysis and which is also predicted by quantum chemical model calculations as the minimum energy conformation, and (ii) as a minority species, which represents a local energy minimum in quantum chemical calculations. The latter conformer has been suggested to be responsible for the "blue" fluorescence showing-up in (moderately) polar solvents next to the polarity-dependent "red" CT fluorescence.

In the directly coupled dyad, which lacks the two single bonds between the bridging phenyl ring and the donor and acceptor species, respectively, as source for geometrical heterogeneity, we observe a similar fluorescence behavior as in the case of the bridged systems studied previously. We therefore present in this contribution the results of steady state and time- and wavelength-resolved fluorescence measurements and discuss the photophysical and photochemical properties of the pheno-

* To whom correspondence should be addressed. E-mail: schneider@chemie.uni-erlangen.de. Phone: +49 9131 8527341. Fax: +49 9131 8528307.

[†] Institut fur Physikalische und Theoretische Chemie.

[‡] Computer-Chemie-Centrum.

10.1021/jp036250u CCC: $25.00
Published on Web 10/18/2003

thiazine−pyrene dyad by comparison with the results of quantum chemical model calculations.

2. Materials and Methods

2.1. Materials. The synthesis of the compound investigated has been described in detail elsewhere.[17,20] The usual analytical techniques were employed to test the purity of the samples. No indication for the presence of impurities or unreacted starting materials could be found. All solvents were spectroscopic grade and used as supplied (Aldrich). Sample solutions (the concentration of the solutes was typically $\leq 5 \times 10^{-5}$ M to avoid excimer formation) were freed from oxygen by bubbling through with argon for about 20 min prior to fluorescence measurements at $T = 298$ K.

2.2. Experimental Methods. UV/vis absorption spectra were recorded on a Perkin-Elmer Lambda 2 spectrometer, and steady-state emission spectra were recorded at ambient temperature on a Perkin-Elmer LS 50B or on a Jobin Yvon Fluoromax 3.

The time- and wavelength-resolved fluorescence experiment employed a setup developed originally by EuroPhoton[21] (Berlin, Germany) but modified by us to suit our specific needs better. Details on the experimental setup are given in refs 18 and 22. Single- and multi-curve fitting[23] was performed in the usual manner employing least-squares fitting techniques based on the Marquardt and Simplex algorithms.[24] The recorded fluorescence intensity distribution I_F (λ_j,t) represents the convolution of the excitation profile $E(t)$ with the fluorescence decay law R (λ_j,t)

$$I_F(\lambda_j,t) = E(t - t_0) \otimes R(\lambda_j,t)$$

where t_0 represents a possible shift of time zero when the scattering solution and sample are exchanged. In the assumed multiexponential decay law

$$R(\lambda_j,t) = \sum A_i(\lambda_j) \exp(-t/\tau_i)$$

$A_i(\lambda_j)$ represents the amplitude of the ith lifetime component for detection wavelength λ_j.

For excitation at $\lambda_{ex} = 277$ nm, the frequency-tripled output of a home-built Titan:sapphire laser[25] with cavity-dumper pumped by a Millennia cw Nd:YAG laser (Spectra Physics) was used ($t_p \approx 100$ fs, repetition rate 800 kHz). Standard NIM electronic components were used in the detection circuit. The system response function measured via scattering of the laser pulse is determined by that of the MCP photomultiplier and showed about 50 ps full-width at half-maximum. Generally, 10^7 fluorescence events were monitored per measurement.

Fluorescence measurements at an elevated pressure were performed with a home-built optical high-pressure cell with windows at 0, 90, and 180°.[22] Fluorescence is detected under 90° through an analyzer set at the magic angle. The sample is contained in a quartz tube and separated from the surrounding pressure medium by a movable Teflon piston.

2.3. Quantum Chemical Model Calculations. Calculations were performed using the program package VAMP 8.0.[26] Molecular properties in the electronic ground state were computed using the restricted Hartree−Fock formalism with the AM1 Hamiltonian.[27] Excited-state calculations used a singles plus pair doubles (PECI)[28] configuration interaction (CI) expansion with an active window of the four highest occupied and the four lowest unoccupied molecular orbitals. Test calculations with both full CI using the same active orbital window and with a singles-only CI with up to 24 active orbitals suggested that this level of theory is adequate for the problem. Excited-state geometries were optimized in vacuo using analytical CI gradients.[29] In some cases, the charge-transfer states were separated energetically from local excitations by applying a homogeneous electrostatic field during the early stages of the geometry optimizations in order to avoid state-crossings during the optimization. Final optimizations were performed without external fields. Solvent effects were simulated in single-point calculations on the gas-phase optimized geometries using our polarized continuum solvation model[30,31] with natural atomic orbital-point charge (NAO−PC) electrostatics,[32] but without the dispersion contribution reported originally.[30] The self-consistent reaction field calculations used solvent-excluded surfaces[33] with atomic radii equal to 120% of those given by Bondi.[34]

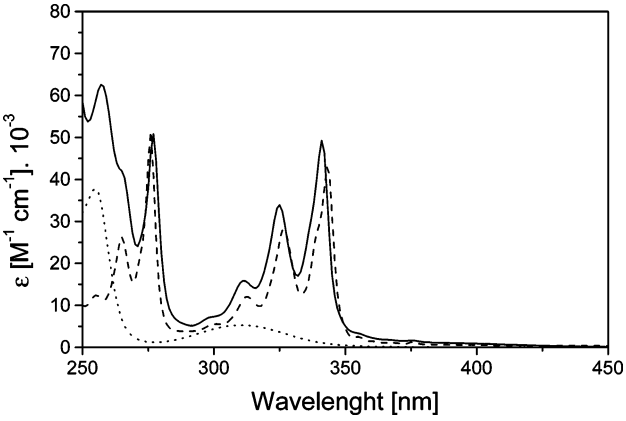

Figure 1. UV/vis absorption spectra of methylpyrene **1b** (- - -), methylphenothiazine **2** (···), and the phenothiazine-pyrene-dyad **3** (—) in methylcyclohexane (MCH).

SCHEME 1: Chemical Structures of Compounds Referred to and Abbreviations Used

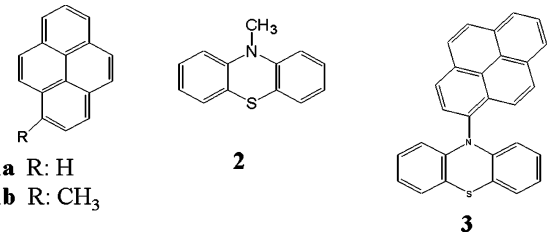

1a R: H
1b R: CH_3

2

3

3. Results

3.1. Steady-State UV/vis Absorption and Emission Spectra. Because of the repulsive interaction of the hydrogen atoms attached to C_{21} and C_{20} of pyrene and C_{14} and C_6 of phenothiazine, one can expect the molecular planes of pyrene and phenothiazine to be essentially orthogonal to each other in dyad 3 (Scheme 1).

Consequently, the conjugation between the two corresponding π-electronic systems is very small, and the UV/vis absorption spectrum of dyad 3 should match the superposition of the absorption spectra of its constituent components (Figure 1).

To take into account the effect of symmetry reduction on transition dipole moments, we have chosen as reference compounds methylpyrene 1b and *N*-methylphenothiazine 2. The absorption spectrum of dyad 3 exhibits a very pronounced vibronic structure below 350 nm like methylpyrene. The maxima are shifted slightly thereby providing evidence for a weak interaction between the two π-electronic systems. The 0−0 transition to the first excited electronic state of (methyl-) pyrene is found at about 376 nm (E_{00} =3.28 eV) and exhibits a very low oscillatory strength only (Table 1).

The absorption spectrum of *N*-methylphenothiazine shows, in the same spectral region, a very broad band of low intensity

TABLE 1: Absorption and Emission Characteristics of Compounds Investigated (Solvent MCH)

	1a	1b	2	3
$E(S_0 \rightarrow S_1)$ nm/eV	372/3.32	376/3.28	382/3.23	376/3.28
$\epsilon_{max} \times 10^3 (S_0 \rightarrow S_1)$ M^{-1} cm^{-1}	0.5	1.2	0.088	1.6
ϕ_F (λ_{ex})	0.26 (300 nm)	0.14 (302 nm)	0.0073 (327 nm)	0.026 (303 nm) (425−650 nm)[a]
ϕ_F (λ_{ex})				0.032 (373 nm) (425−650 nm)[a]
ϕ_F (λ_{ex})				0.0062 (299 nm) (350−437 nm)[a]

[a] Wavelength range of integration.

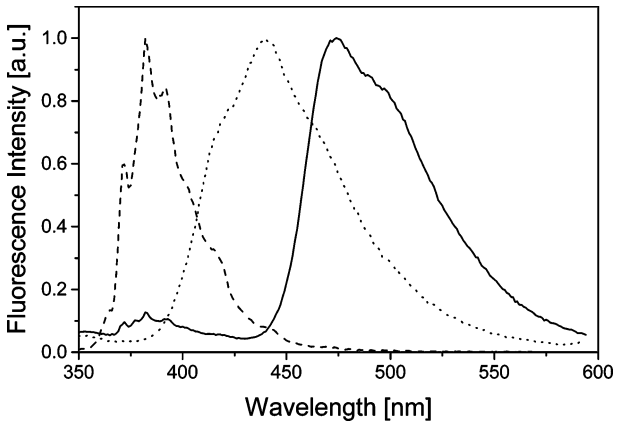

Figure 2. Normalized steady-state fluorescence spectra of **1a** (- - -), **2** (···). and **3** (—) (λ_{ex} = 300 nm) in methylcyclohexane.

($\lambda_m \sim 312$ nm). An estimation of its 0−0 transition energy is difficult. By comparison with the absorption and fluorescence spectra of *N*-phenylphenothiazine, we adopt a value of E_{00} = 3.23 eV (382 nm).

The absorption spectra of the constituent components also suggest that, with an excitation wavelength $\lambda_{ex} \sim 300$ nm, the excitation light is absorbed by both components with roughly equal probability. For excitation wavelength $\lambda_{ex} \sim 340$ or 275 nm, the exciting light is nearly exclusively absorbed by the pyrene chromophore.

It should be mentioned that the absorption spectra of methylpyrene and *N*-methylphenothiazine exhibit only a weak solvatochromism. The position of the vibrational bands observed in the pyrene $S_0 \rightarrow S_2$ absorption band varies by a few nanometers if dyad 3 is dissolved in different solvents.

The emission spectrum of dyad 3 ($\lambda_{ex} \sim 300$ nm) in MCH solvent shows two contributions, a "blue" fluorescence component that exhibits a weak vibronic structure like the fluorescence spectrum of pyrene and a "red" fluorescence component without any indication of vibrational structure ($\lambda_m \sim 470$ nm), but with a long wavelength tail extending beyond 600 nm (Figure 2).

Because we found that the vibrational structure of the fluorescence of pyrene resembles more closely the vibrational structure of the "blue" emission of dyad 3, we display its fluorescence spectrum rather than that of methylpyrene for comparison in Figure 2. (This procedure also facilitates the determination of relative fluorescence yields.) The fluorescence spectrum of *N*-methylphenothiazine, which exhibits a very broad and nearly structureless distribution with a maximum around 440 nm, is also shown. Because of the difference in the location of the maxima, we must conclude that with excitation wavelength λ_{ex} = 300 nm no clear evidence is found in the emission spectrum of dyad 3 for fluorescence from a locally excited (LE) state of phenothiazine. The "red" emission of dyad 3 should, therefore, represent fluorescence from a charge transfer (CT) state. Its fluorescence yield amounts to about 0.032 (Table 1).

Methyl substitution reduces the fluorescence quantum yield of pyrene in MCH by approximately a factor of 2 (0.14 versus 0.26). Upon excitation around 300 nm, where pyrene and phenothiazine absorb light about equally well, the fluorescence yield of the "blue" emission is reduced to about 0.006. If it only represented pyrene emission, this result would indicate that the fluorescence quantum yield of the pyrene moiety is reduced by a factor of about 15−20 by additional radiationless decay channels opened up in the dyad. The fluorescence yield of the "red" emission determined upon short wavelength excitation amounts to about 0.026. If one assumes a quantum yield of about 90% for the formation of the CT state upon excitation of pyrene, then one would estimate a quantum yield of CT fluorescence on the order of 0.03.

A widely used criterion to identify emission from a charge transfer state is a strong solvatochromism. Therefore, we show the emission spectra of dyad 3 in dependence on the excitation wavelength for the solvents methylcyclohexane (Figure 3A), methylenechloride (Figure 3B), and acetonitrile (Figure 3C).

In methylcyclohexane, the emission is generally dominated by a fluorescence component ($\lambda_m \sim 475$ nm), whose spectral distribution is nearly independent of the excitation wavelength. Especially noteworthy is that excitation into the long wavelength tail around 400 nm yields the same fluorescence spectrum. This suggests that the long wavelength tail may actually represent a very weak CT absorption. Furthermore, one finds that even for those excitation wavelengths for which the extinction is governed by the absorption of pyrene, the "blue" contribution to the fluorescence is very weak.

In acetonitrile (ACN), the fluorescence spectrum of dyad 3 exhibits three distinct contributions. For short wavelength excitation, a "blue" contribution with vibrational structure as known from pyrene is seen. [Remember that the relative intensities of the vibrational pattern of the pyrene fluorescence vary with solvent polarity. Note also that in the recorded spectra three Raman bands can show up. Two bands originate from the solvent ($\Delta\tilde{\nu}$(CH) ≈ 2950 cm^{-1} and $\Delta\tilde{\nu}$(CN) ≈ 2250 cm^{-1}) and one (resonance-enhanced) from pyrene ($\Delta\tilde{\nu} \approx 1400$ cm^{-1}).] The intensity of the "blue" emission measured relative to that of the broad and structureless fluorescence from the CT state ($\lambda_m \sim 608$ nm) varies strongly with the excitation wavelength. Interestingly, it is fairly strong if the excitation wavelength is chosen around 300−315 nm, where phenothiazine and pyrene absorb equally well. In contrast, for λ_{ex} = 277 or 345 nm, where the extinction is dominated by that of pyrene, the pyrene type emission is again fairly weak, as in the MCH solvent. Between the pyrene type fluorescence and the CT fluorescence, one finds a third component with a broad and structureless spectrum ($\lambda_m \sim 445$ nm). Its relative intensity increases with longer excitation wavelength. This and the location of the maximum suggest that it could be emission from an LE state of phenothiazine.

In a solvent of medium polarity, like CH_2Cl_2, the broad and structureless "red" fluorescence component is less bathochromically shifted than in acetonitrile ($\lambda_m \sim 580$ nm). Its spectral distribution is again independent of excitation wavelength. However, in contrast to the spectrum recorded in MCH or ACN,

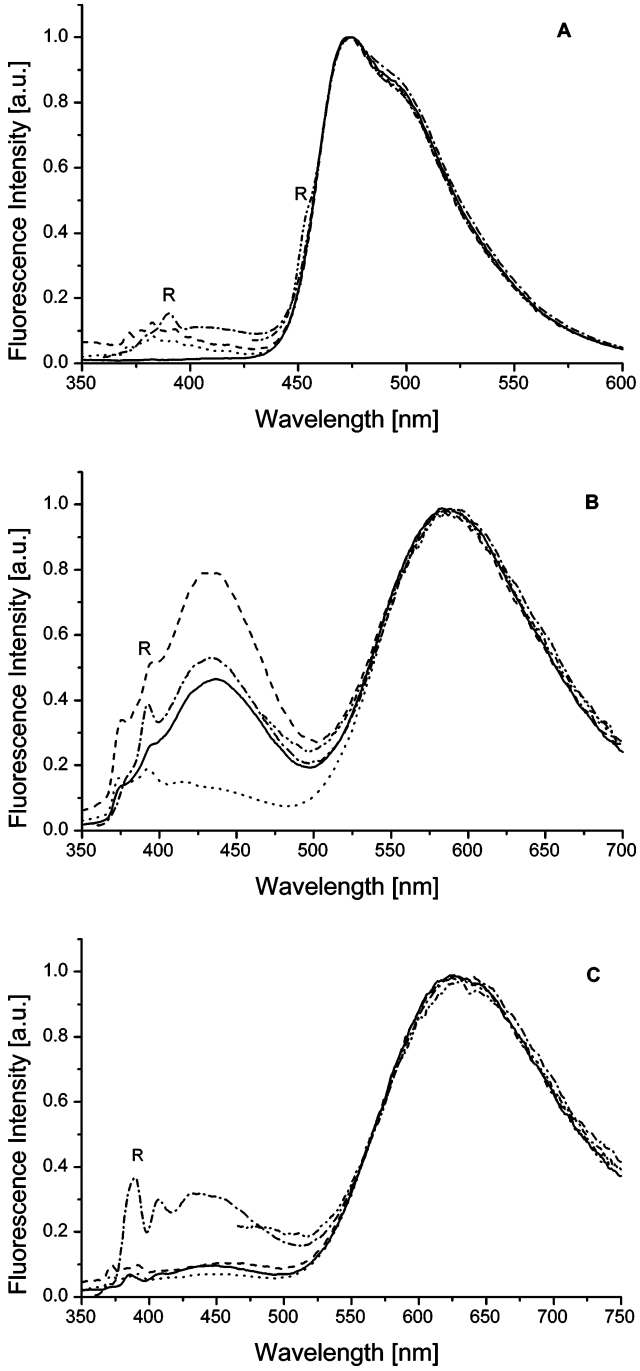

Figure 3. Excitation wavelength dependence of the steady-state fluorescence spectra (normalized) of compound **3** in (A) MCH, (B) CH_2Cl_2, and (C) acetonitrile (ACN). λ_{ex}: 277 (—), 300 (- - -), 310 (···), 350 (-·-), and 400 nm (-···-). R denotes Raman band.

no shoulder appears on the long wavelength side. If the excitation wavelength is chosen to match the onset of the strong absorption band ($\lambda_{ex} \sim 350$ nm), one finds a broad and structureless fluorescence band again. Its maximum is now around 430 nm, and one could question whether it represents an LE emission of phenothiazine. At even shorter excitation wavelength, a third fluorescence component appears with some vibrational structure indicated. The positions of the maxima are in accord with an assignment to emission of pyrene.

To get an estimate on the dipole moment of the charge transfer state formed in dyad 3, we constructed a Lippert−Mataga plot using the maxima of the CT fluorescence in solvents of different polarity.[35] In Figure 4, two different fits are shown: The first fit includes all data points, and the second fit

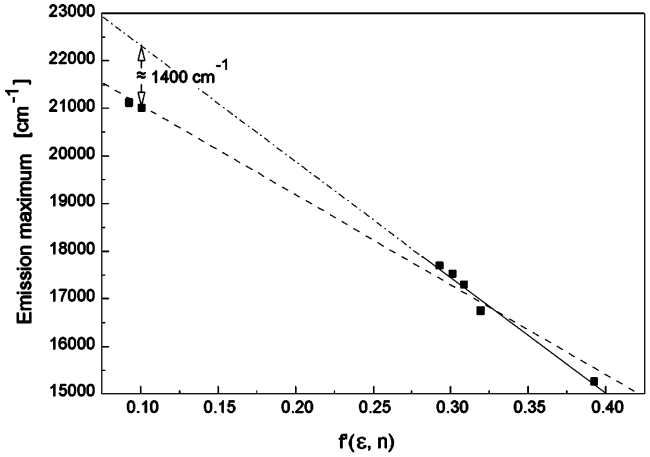

Figure 4. Lippert−Mataga plot of the CT fluorescence emission maxima of **3** in different solvents (*n*-hexane, cyclohexane, ethyl acetate, Me-THF, THF, CH_2Cl_2, and acetonitrile). $f' = (\epsilon - 1)/(2\epsilon + 1) - 0.5(n^2 - 1)/(2n^2 - 1)$. The data points collected for nonpolar solvents is omitted in one of the linear fits because of reasons discussed in the text.

ignores the points obtained in solvents with f' below 0.2. In the latter case, the remaining data points are well reproduced, and the slope is significantly higher.

Accordingly, the expected transition energy in MCH is about 1400 cm^{-1} higher than the experimental value. Based on our experience[11] and that of other groups,[12] we interpret this deviation as evidence for a different geometry of the CT state in nonpolar and polar solvents. To corroborate this hypothesis, we recorded steady-state fluorescence spectra in MCH under pressures up to 3500 bar (Figure 5a).

Three observations are remarkable: (i) The intensity-normalized CT fluorescence spectrum exhibits a continuous red shift with increasing pressure (increasing solvent polarity) without changing the spectral distribution. (ii) The relative intensity of the shorter wavelength emission ($\lambda_m \sim 390$ nm) increases steadily with pressure. (iii) In the presentation chosen, there seems to exist an isoemissive point at $\lambda \sim 442$ nm. In accordance with the above-described finding, no indication of pyrene-type emission is found for the excitation wavelength employed (309 nm).

By using published data of the pressure dependence of refractive index *n* and dielectric constant ϵ of MCH,[36] we can calculate the f' values needed for a Lippert−Mataga plot. Although the range of f' values covered is small, we have the advantage that no variations in solute−solvent interaction occur as experienced when the nature of the solvent is changed. Therefore, it is not surprising that the slope of the correlated Lippert−Mataga plot (Figure 5b) is well determined. It is about 24% lower than that obtained from the data collected in polar solvents (see also Table 8).

If one applies the Onsager model and assumes the same value for the radius of the cavity, *a*, this result can be taken as clear evidence for a different (geometry of the) CT state in nonpolar versus polar solvents.

The finding that the relative intensity of "blue" versus "red" fluorescence varies strongly with excitation wavelength manifests itself more clearly in the fluorescence excitation spectra monitored for the different spectral regions. If the fluorescence of the CT emission in CH_2Cl_2 is recorded ($\lambda_{det} = 600$ nm), the excitation spectra show a continuous, slow rise, starting from about 480 nm; the slope increases strongly shortly before the first maximum is reached at about 342 nm (Figure 6A). (Note again that some of the small peaks observed in the excitation

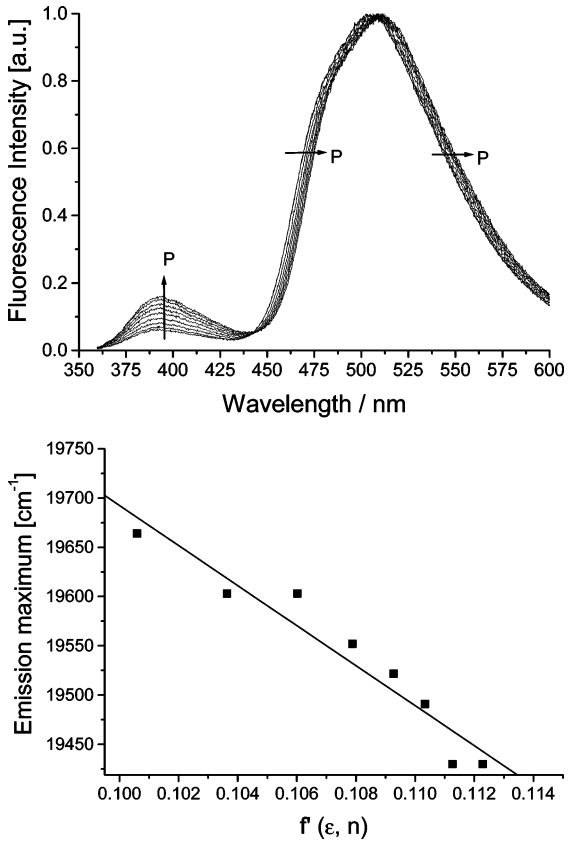

Figure 5. Pressure dependence of the normalized steady-state fluorescence (top) of **3** in MCH, $\lambda_{ex} = 310$ nm. Arrows indicate increasing pressure. Lippert−Mataga plot (bottom) derived from the data presented in top part for **3**. (ϵ values are taken from ref 36.)

TABLE 2: Photophysical Parameters Determined for Dyad 3 from Time- and Wavelength-Resolved Fluorescence Measurements ($\lambda_{ex} = 277$ nm)[a]

solvent	property	**3**	solvent	property	**3**
cyclohexane	τ(CT)/ns	3.7	CH_2Cl_2	τ_2(LE)/ns	67
	λ_{em}/nm	450		λ_{em}/nm	400
	τ(LE)/ns	100	acetonitrile	τ(CT)/ns	6.0
	λ_{em}/nm	400		λ_{em}/nm	640
CH_2Cl_2	τ(CT)/ns	5.8		τ_1(LE)/ns	12
	λ_{em}/nm	560		λ_{em}/nm	460
	τ_1(LE)/ns	9.3		τ_2(LE)/ns	110
	λ_{em}/nm	440		λ_{em}/nm	410

[a] λ_{em} refers to the maximum in the decay associated spectra of the corresponding lifetime component.

spectra can be artifacts caused by Raman scattering. They show up only if the fluorescence intensity is very small as in case of dyad 3.)

In the following decrease, one observes a vibronic structure as known from the absorption spectra. A further maximum found at about 277 nm is evidence for a higher excited state. The locations of both maxima coincide with the positions of maxima found in the absorption spectrum.

If, on the other hand, the emission is monitored in the region of the phenothiazine fluorescence ($\lambda_{det} \cong 450$ nm), the increase in the excitation spectra starts around 450 nm. The first maximum is reached at about 347 nm; it is followed by several well-separated maxima of lower intensity. Noteworthy are the appearance of an additional maximum around 300 nm and the bathochromic shift of the short-wavelength peak from 280 to 283 nm.

If the detection wavelength is chosen to coincide with the fluorescence maximum of the pyrene moiety at 392 nm, then

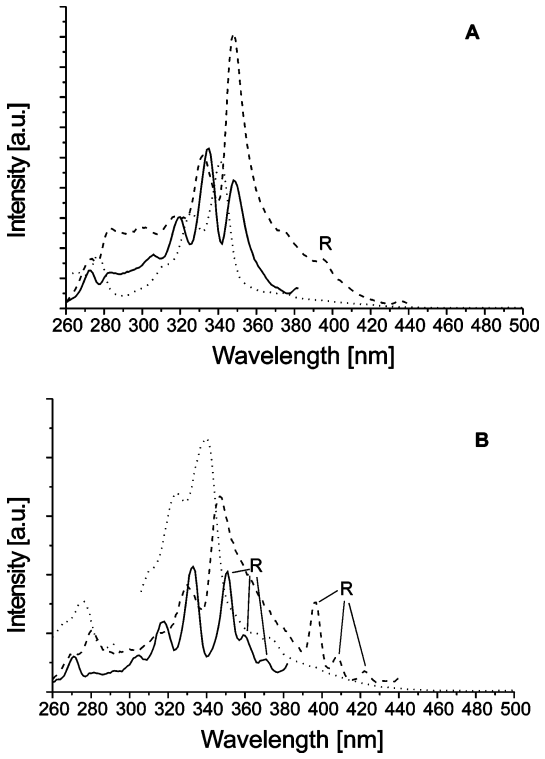

Figure 6. Fluorescence excitation spectra of dyad **3** in CH_2Cl_2 (A) and acetonitrile (B) recorded with different detection wavelengths: 600 (...), 450 (- - -), and 392 (—) nm. R denotes Raman bands.

the vibrational structure is well expressed in the excitation spectra, but the most intense peak is now the second one at about 336 nm. Similarly, the intensity ratio of the peaks at about 275 and 283 nm is inverted versus that with 450 nm detection wavelength.

The excitation spectra recorded for dyad 3 in acetonitrile corroborate the findings described above for CH_2Cl_2 as solvent. Especially the bathochromic shift of the peaks by several nanometers is reproduced, if the emission is monitored in the "blue" spectral region.

The excitation spectra recorded in solvents of medium and high polarity, therefore, provide clear evidence that the "blue" and "red" fluorescence originate from two different species, which exhibit absorption spectra with similar features. The spectrum of the species emitting the "blue" fluorescence is bathochromically shifted by several nanometers. The excitation spectrum of the species, which forms readily the CT state, matches closely the absorption spectrum recorded for dyad 3. In accordance with the results obtained by time-resolved transient absorption and time-resolved resonance Raman spectroscopy, we may conclude that the latter species should be present in excess, whereas the "blue" emitting species should be present as a minority species. In view of the similar features of the absorption spectra, we propose, as in the case of the phenyl-bridged systems studied previously, that the two emitting species represent isomeric forms.

3.2. Time- and Wavelength-Resolved Fluorescence Spectroscopy. The time- and wavelength-resolved fluorescence decay curves recorded for dyad 3 provide direct evidence that the "blue" and "red" emission bands appear immediately after excitation without any measurable delay. For the "red" emission, this finding is in accordance with the results of the pump−probe experiments, which yielded electron-transfer rates on the order of $k_{et} \approx 10^{11}$ s^{-1}.

The analysis of the temporal fluorescence profiles recorded in the farmost red spectral range showed that the CT fluores-

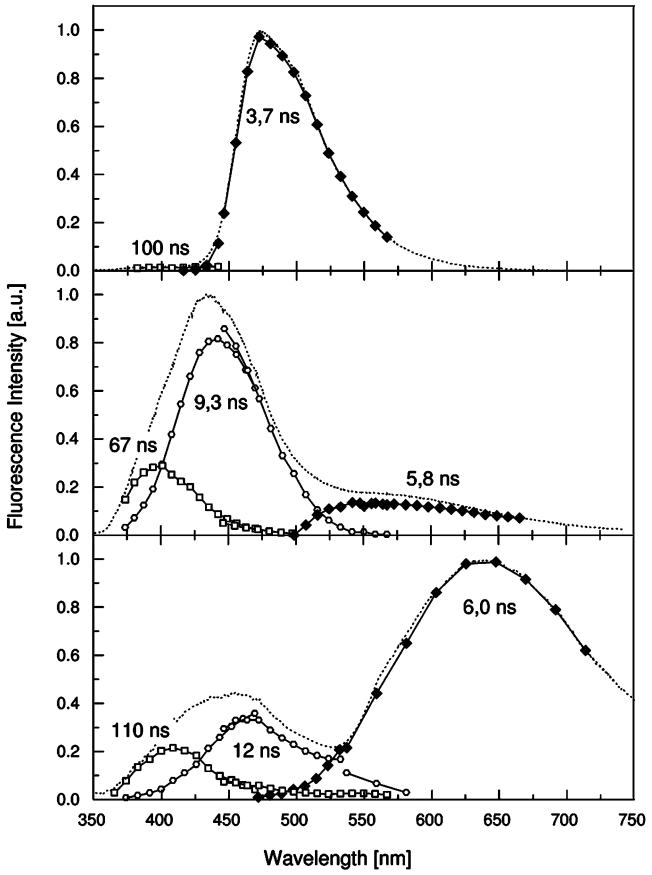

Figure 7. Decay associated spectra (DAS) obtained for **3** in different solvents with $\lambda_{ex} = 277$ nm: (top) cyclohexane, (middle) CH_2Cl_2, and (bottom) acetonitrile. The spectrograph settings were chosen to yield overlapping spectral regions.

cence decays monoexponentially with decay times varying between 3.7 (cyclohexane) and 6.0 ns (acetonitrile), Table 2.

In the spectral range of the "blue" emission, a proper fit of the fluorescence time profiles needed two exponentials. If the spectrally corrected steady-state emission spectra recorded for the same excitation wavelength are used in addition, one can construct the decay associated spectra (DAS) according to

$$\mathrm{DAS}(\lambda_j,\tau_i) = \frac{A_i(\lambda_j)\tau_i}{\sum A_i(\lambda_j)\tau_i} F(\lambda_j)$$

where $F(\lambda_j)$ represents the steady-state spectral distribution and A_i and τ_i are the parameters derived by the global fit procedure for the assumed multiexponential fluorescence decay law $R(\lambda_j,t)$

$$R(\lambda_j,t) = \sum_{i=1}^{3} A_i(\lambda_j)\exp(-t/\tau_i)$$

The decay-associated spectra calculated for the various fluorescence components found in CH_2Cl_2 and acetonitrile exhibit interesting features with respect to spectral distribution (Figure 7).

The maximum of the DAS of the longest-lived component ($\tau > 60$ ns) is at about the same wavelength in both solvents, around 400 nm. It matches well the fluorescence maximum of (phenyl-) substituted pyrene, whose fluorescence spectrum shows only a weak vibrational structure. It appears, however, that the long wavelength tail extends further to the red. Furthermore, the decay times determined are pronouncedly shorter than those of pyrene or its methyl or phenyl derivatives. The DAS of the second fluorescence component peaks around 450 nm in fair agreement with the maximum of the phenothiazine fluorescence. In acetonitrile, the peak position is slightly shifted to a longer wavelength. This explains why the spectrum of the "blue" component is broader in the steady-state spectrum.

In conclusion, the differences between the fluorescence lifetimes of the model compounds 1 and 2 and the lifetimes determined by the analysis of the "blue" emission of dyad 3 contradict a suggestion that the latter is caused by traces of pyrene or phenothiazine.

The DAS of the shortest-lived component supports the assumption that the "red" fluorescence originates from one emitting CT state only. The apparent increase in decay time with increasing solvent polarity (and concomitantly reduced energy gap to the electronic ground state) represents an unusual behavior. It can be taken as a hint that radiationless deactivation to the electronic groundstate is not the only or dominant relaxation process of dyad 3 in all solvents employed.

In addition to the time-resolved fluorescence measurements at ambient pressure, we also recorded fluorescence decay curves in MCH at pressures up to 3500 bar. The fluorescence-decay curves ($\lambda_{det} \approx 470$ nm) can be fitted very well with one single exponential for pressures up to 2500 bar (an example is shown in Figure S1 of the Supporting Information).

The decay time varies only slightly with pressure from 3.82 ns (1 bar) via 3.75 ns (1000 bar) to 3.72 ns (2000 bar). For pressures above 2500 bar, a biexponential decay law is needed for an optimum fit. At 3000 bar, the longer lifetime is still about 3.70 ns; the second component exhibits a decay time of about 1.23 ns with a relative amplitude of about 1.5%.

That the lifetime of the CT fluorescence is essentially independent of pressure is astonishing in view of the fact that the intensity measured in the steady-state experiment decreases by a factor of 0.7 for the increase of pressure from 1 to 1500 bar. This, together with the increase of the relative intensity of the "blue" fluorescence component, could indicate that the efficiency of the charge-transfer process varies with pressure. Alternatively, a pressure increase could change the equilibrium distribution between the two postulated isomers or, at least, the contribution $\epsilon_i c_i$ of each isomer to the total extinction at the excitation wavelength. In contrast, we found empirically that the recorded fluorescence intensity of methylpyrene increased by more than a factor of 2 in the quoted pressure range.

3.3. Calculated Geometries and Excitation Energies for Dyad 3. The semiempirical calculations employing the AM1 Hamiltonian produce an energy-minimized structure for dyad 3, in which the phenothiazine is slightly bent along the axis S−N (angle β in Table 3). As a consequence, a differentiation of conformers is possible depending on the orientation of the pyrene moiety. According to the calculations, and perhaps in agreement with intuition, the pyrene moiety is located on the convex side of the phenothiazine fragment in the most stable conformer 1 (pictures of the calculated geometries are displayed in Figure S2 of the Supporting Information).

The single bond connecting phenothiazine and the pyrene moiety is rotated by about −103° (angle α in Table 3) and thus allows some conjugation between the two π-electronic systems.

In the search for the second, metastable conformer, we used a starting geometry derived from the most stable one by rotation of the single bond N10−C15 by 180° (Figure S2 of the Supporting Information). This means that the center of gravity of the pyrene moiety lies on the concave side of phenothiazine. The search for the closest local minimum on the energy

TABLE 3: Calculated Parameters of the Two Conformers of Dyad 3 in the Ground State (GS) and in the Relaxed Excited States S_1 and S_2, Respectively

	isomer 1			isomer 2		
parameters	GS	S1 (relaxed)	S2 (relaxed)	GS	S1 (relaxed)	S2 (relaxed)
α (°)	−102.9	−93.2	−64.4	81.9	91.5	63.9
β (°)	154.2	175.6	178.7	150.4	175.8	176.2
μ (D)	2.19	0.53	11.4	2.57	0.52	8.23
ΔH_f(kJ/mol) vacuum	623	871.9	951.5	625	871.9	952.3
R_{DA}(Å)[a]	5.78	5.82	5.85	5.89	5.82	5.85
ΔH_f(kJ/mol) acetonitrile	606.5			608		

[a] R_{DA} represents distance between the centers of phenothiazine and pyrene in both conformers.

TABLE 4: Excited State Properties Predicted by Quantum Chemical Model Calculations for Dyad 3 (Conformer 1 in Vacuo, PECI = 8)[a]

state	ΔE, eV	λ_{ex}, nm	f	$\Delta\mu$, D	character	predominant transitions
S1	2.97	417	0.002	2.89	LE Phtz	H → L+2
						H−2 → L+3
S2	3.61	344	0.170	0.62	LE Py	H−1 → L
						H−3 → L+1
						H−1 → L+1
S3	3.63	342	0.025	0.96	LE Py	H−1 → L+1
						H−1 → L
						H−3 → L
S4	3.87	320	0.181	4.34	LE Phtz + CT	H → L+3
						H → L
						H−2 → L+2
S5	3.97	313	0.008	24.6	CT + LE Phtz	H → L
						H → L+3
						H−2 → L
S6	4.73	262	0.0	26.99	CT	H → L+1
						H−2 → L+1
T1	2.65	466			LE Phtz	H → L+2
T2	2.69	459			LE Py	H−1 → L

[a] The MOs involved in the description of the 8 lowest excited state are shown in Figure S3 of the Supporting Information.

TABLE 5: Excited State Properties Predicted by Quantum Chemical Model Calculations for Dyad 3 (Conformer 2 in Vacuo, PECI = 8)

state	ΔE, eV	λ_{ex}, nm	f	$\Delta\mu$, D	character	predominant transitions
S1	2.92	425	0.001	2.85	LE Phtz	H → L+2
S2	3.61	343	0.183	0.30	LE Py	H−1 → L
						H−3 → L+1
						H−1 → L+1
S3	3.64	341	0.012	0.57	LE Py	H−1 → L+1
						H−3 → L
						H−1 → L
S4	3.83	324	0.044	19.67	CT + LE Phtz	H → L
						H → L+3
						H−2 → L
S5	3.91	317	0.141	10.28	LE Phtz + CT	H → L+3
						H → L
						H−2 → L+2
S6	4.65	267	0.003	26.98	CT	H → L+1
						H−2 → L+1
T1	2.59	476			LE Phtz	H → L+2
T2	2.69	459			LE Py	H−1 → L

hypersurface yields conformer 2, which is by about 1.7 kJ/mol less stable than conformer 1. Assuming equivalent contributions of the entropy to the Gibbs energy, the calculations predict an equilibrium population of the two isomers of about 2:1. In the energy optimized conformer 2, the single bond is rotated by 82°, indicating a slightly different interaction between the pyrene and phenothiazine moiety in the two conformers.

A significant difference is also found in the degree of bending of phenothiazine as expressed by the angle C4C5N10C9 (154° versus 150°). The modifications of the phenothiazine geometry also lead to a small change of the dipole moment calculated for the electronic ground states (2.19 versus 2.57 D), because the change in hybridization of the nitrogen changes its ionization potential and concomitantly its donor properties.

As may be expected, the quantum-chemical calculations (gas phase) yield slightly different molecular orbital schemes for the two conformers (a graphic representation of the MOs of conformer 1 is given in Figure S3 of the Supporting Information).

In both conformers, the HOMO and LUMO are strongly localized on phenothiazine (donor) and pyrene (acceptor), respectively. According to the common, but oversimplified, one-electron concept, the HOMO → LUMO transition would represent an essentially complete charge-transfer excitation with a very low extinction coefficient. The CI calculations predict that the HOMO → LUMO transition dominates the CI description of the S_5 state of conformer 1 and, consequently, causes a large change in dipole moment upon transition to this state (Table 4).

Because the LUMO + 1 orbital is also completely localized on the pyrene part, the HOMO → LUMO + 1 transition, which dominates the $S_0 \rightarrow S_6$ excitation, represents a second, higher lying CT excitation. The connected change in dipole moment is even higher (27 D) than that connected with $S_0 \rightarrow S_5$ excitation (24.6 D).

However, in conformer 2, the HOMO → LUMO one-electron excitation dominates the CI description of S_4. Because some phenothiazine-localized excitation is mixed in, $S_0 \rightarrow S_4$ excitation results in a change of the dipole moment of only 19.7 D (Table 5).

A smaller, but still significant change of the dipole moment is connected with the $S_0 \rightarrow S_5$ transition (10.3 D), because the CI description is dominated by a local excitation of phenothiazine (HOMO → LUMO+3) with some contribution of HOMO → LUMO one-electron excitation. The HOMO → LUMO + 1 one electron excitation dominates in the description of S_6. The $S_0 \rightarrow S_6$ excitation is again connected with a change of dipole moment of 27 D. To gain a better insight into the net charge distribution of the two excited states with large dipole moment, the molecular electrostatic potentials are compared in Figure S4 of the Supporting Information. The spatial distributions of the positive and negative excess charges are very similar in both CT states, only the amount of charge transferred is slightly higher in the S_6 state.

In both conformers, the one-electron promotion from HOMO − 1 or HOMO − 3 to LUMO contributes to locally excited states of pyrene. The latter transitions (including those to LUMO + 1) establish the second excited state with a fairly large oscillator strength f and the nearly isoenergetic state S_3 with lower oscillator strength. The same wrong sequence is obtained for the parent pyrene, because the $S_0 \rightarrow S_1$ transition is actually

TABLE 6: Calculated Properties (SCRF model) of Electronically Excited States of Dyad 3 (Conformer 1) in Acetonitrile ($\epsilon = 37$)

state in vacuo	state in ACN	ΔE, eV	λ_{ex}, nm	f	$\Delta\mu$, D	character	predominant transitions
S1	S1	3.05	406.9	0.0	2.71	LE Phtz	H → L+2
							H−2 → L+3
S2	S2	3.59	345.1	0.154	0.64	LE Py	H−1 → L
							H−3 → L+1
							H−1 → L+1
S3	S3	3.62	342.4	0.041	0.98	LE Py	H−1 → L+1
							H−3 → L
							H−1 → L
S4	S5	3.98	311.6	0.176	0.93	LE Phtz	H → L+3
							H−2 → L+2
S5	S4	3.81	325.3	0.0	25.86	CT	H → L
							H−2 → L
S6	S6	4.51	275.2	0.001	26.67	CT	H → L+1
							H−2 → L+1
							H → L
T2	T1	2.69	456.7			LE Py	H−1 → L
T1	T2	2.72	453.7			LE Phtz	H → L+2

the extremely weak one. However, this inversion of the two close-lying excited states of pyrene has no real consequence on the following discussion.

The first excited singlet state of the dyad ($\lambda_{ex} = 417$ and 425 nm, respectively) with very low oscillator strength could, according to the calculations, be responsible for a long-wavelength tail in the absorption spectrum of both conformers. It mainly represents the excitation of phenothiazine. Internal conversion from the preferentially excited S_2 state (largest oscillator strength) to the S_1 state would correspond to an energy transfer from pyrene to phenothiazine. Photoinduced formation of a CT state is possible if the CT states as calculated are stabilized enough by interaction with the solvent and/or by structural relaxation so that they lie below the essentially locally excited states of phenothiazine or pyrene. This is likely despite the high energies calculated, because the model calculations in the approximation used tend to overestimate the energy needed for charge separation by up to 0.5 eV.[13c,31,37]

The results shown in Tables 5 and 6 suggest that the rotation of the phenothiazine moiety by about 180° has no significant effect on the three lowest excited states, because these represent local excitations of the phenothiazine and pyrene moieties, respectively. The change in spatial arrangement of the two constituent elements results, however, in a change of the distance across which charge must be transferred when forming a CT state. The connected changes in the electrostatic interaction result in different expansion coefficients of the CI description of the excited states S_4 and S_5 and, consequently, in different values of oscillatory strength and dipole moment. However, the S_6 excited state represents a full CT state in both isomers with an equally large dipole moment (27D).

3.4. Stabilization of CT States by Solvent and Geometrical Relaxation. The only significant difference in the description of the excited states of isomers 1 and 2 appears in the in vacuo calculations for S_4 and S_5. When the SCRF model is applied to simulate the effect of acetonitrile as solvent, the CI description of the excited states becomes very similar for the two isomers (Tables 6 and 7).

The excited states with high dipole moment are uniformly S_5 and S_6. As another consequence, these states exhibit a bathochromic shift on the order of 15 nm. However, because their oscillator strength is negligible, these shifts cannot be detected in the experimental spectra.

To elucidate whether geometrical relaxation processes should occur in the excited states, we employed a recently developed

TABLE 7: Calculated Properties (SCRF model) of Electronically Excited States of Dyad 3 (conformer 2) in Acetonitrile ($\epsilon = 37$)

state in vacuo	state in ACN	ΔE, eV	λ_{ex}, nm	f	$\Delta\mu$, D	character	predominant transitions
S1	S1	2.99	414.0	0.0	2.63	LE Phtz	H → L+2
							H−2 → L+3
S2	S2	3.60	344.5	0.17	0.42	LE Py	H−1 → L
							H−3 → L+1
							H−1 → L+1
S3	S3	3.61	342.0	0.026	0.79	LE Py	H−1 → L+1
							H−3 → L
							H−1 → L
S4	S5	3.94	314.7	0.174	3.46	LE Phtz + CT	H → L+3
							H−2 → L+2
							H → L
S5	S4	3.77	329.0	0.009	25.30	CT + LE Phtz	H → L
							H−2 → L
							H → L+3
S6	S6	4.47	277.1	0.014	26.33	CT	H → L+1
							H−2 → L+1
T1	T1	2.66	463.7			LE Phtz	H → L+2
T2	T2	2.69	458.7			LE Py	H−1 → L

geometry optimization algorithm to search for those molecular geometries, which represent minima on the energy hypersurface of specific excited states (in vacuo). For S_6 of both isomers, the program produces a relaxed CT state geometry in which the phenothiazine moiety is essentially planar and the single bond is rotated by close to 90°. The planarisation is in accord with the well-known fact that upon oxidation the nitrogen in phenothiazine changes to sp^2 hybridization.

Most interesting is, however, that relaxation to nearly the same geometry occurs (Figure 8, top) if one applies the optimization procedure to the first excited singlet state (LE excitation of phenothiazine).

This coincidence allows us to discuss the variation of the energy hypersurface along the same nuclear relaxation coordinate. The energy gained by a structural relaxation in the S_1 state is calculated to be about the same for both isomers, namely approximately 37.6 kJ mol^{-1} or 0.38 eV/molecule (Scheme 2).

Although this amount is larger than the inner reorganization energy of phenothiazine (0.2 eV), as reported by different authors, it nevertheless should be due to the reorganization of phenothiazine only. This hypothesis is supported by the fact that the same geometry optimization procedure applied to *N*-methyl phenothiazine in vacuo produces a stabilization energy of 0.32 eV for the S_1 state and 0.36 eV for the electronic ground state.

A perfect planarisation of the phenothiazine moiety has the effect that the rotation of the single bond by +90° and −90° leads to indistinguishable forms of dyad 3. The small deviations from perfect planarity result in small differences of the calculated energies below the accuracy of the method. However, if one applies the geometry-optimization procedure to the pyrene-localized S_2 state, one obtains a different relaxed geometry (Figure 8, bottom). The phenothiazine moiety adopts a nearly planar geometry as in the cases discussed previously, but the angle of torsion of the single bond is only about 70°. This implies a modified reaction coordinate for the inner reorganization of dyad 3. Because of the near planarity of the phenothiazine moiety, the relaxed geometries calculated for the two isomers under consideration represent approximate mirror images with equivalent excitation energies. Unfortunately, CI gradients are not yet available within the SCRF model. Therefore, our presentation in Scheme 2 is restricted to the in vacuo case.

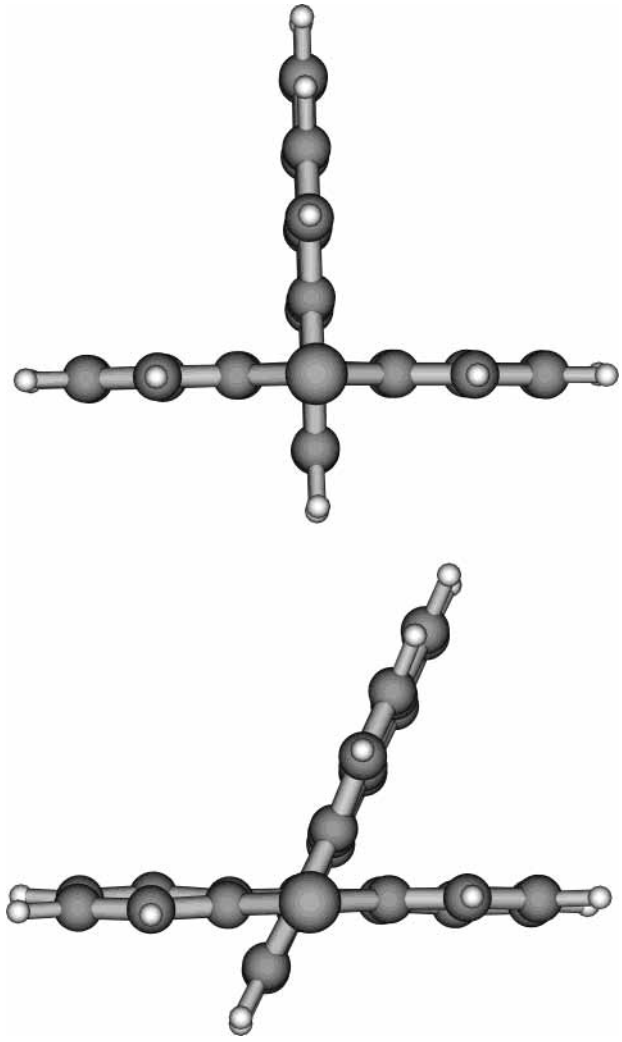

Figure 8. Structures of the two fully relaxed lowest excited singlet states of dyad **3**. Phenothiazine-localized S_1 (top) and pyrene-localized S_2 state (bottom). For more details see text.

SCHEME 2: Comparison of Excited State Energies of Isomers 1 and 2 in Their Ground State Optimized Geometry and in the (Equivalent) Geometry of the Fully Relaxed Excited States (Note that the Latter Geometries Differ for the Different Electronic States)

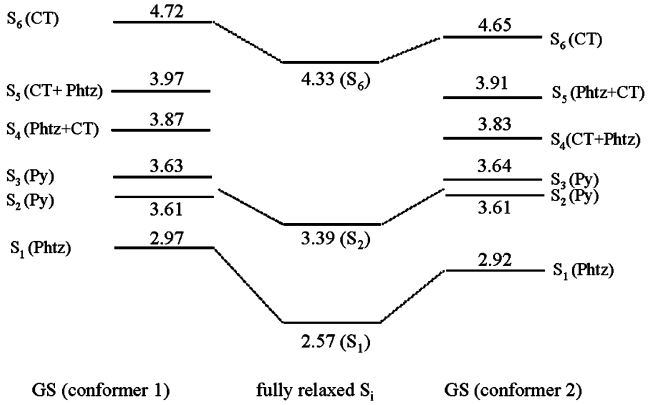

At first thought surprising is that the geometry-optimization algorithm does not work for the S_5 state, whose CI description is dominated by the HOMO → LUMO one-electron transition. This result is, however, in our opinion the important hint for understanding the different photophysical behavior of the two isomers considered (see below).

SCHEME 3: Variation of Calculated Excited State Energies of Conformer 1 in the Franck−Condon State (Ground-State Geometry) and in the Geometry of the Fully Relaxed, Phenothiazine-Localized S_1 (top) and the Fully Relaxed Pyrene-Localized S_2 State (bottom)

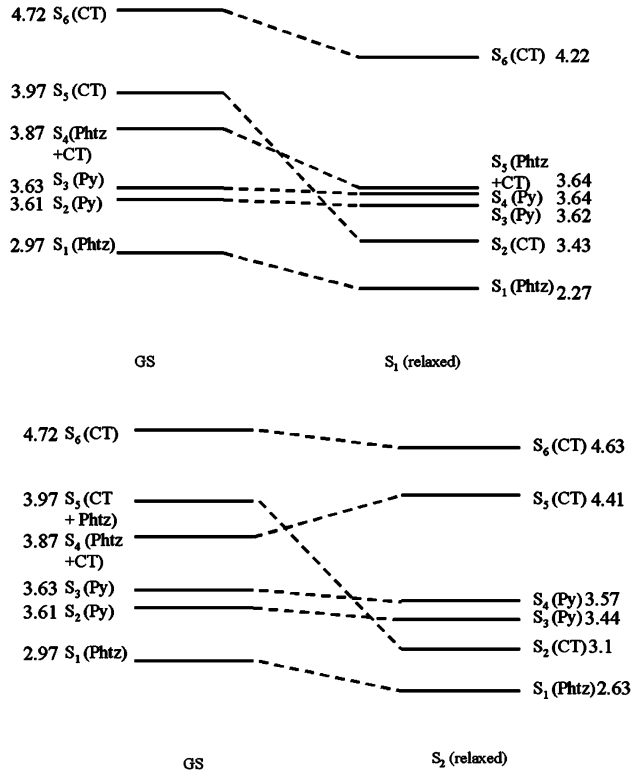

Because the energies of the CT states calculated for the relaxed S_1- and S_2-state geometries are still higher than the energy of the lowest locally excited state, the calculations in vacuo cannot explain the formation of a CT state upon excitation of either phenothiazine or pyrene (Scheme 3).

On the other hand, it is known that this type of calculation tends to overestimate the energy needed for charge separation. Therefore, we will attempt to make an alternative estimate of the energy of the fluorescing CT state.

3.5. Alternative Estimates of the Energy of the Fluorescing CT State. If the structure of the electron donor−acceptor system in the CT state is known, one can estimate the change in Gibbs energy upon formation of the CT state, ΔG_{CT}, via the Weller equation[38]

$$\Delta G_{CT} = e(E_{ox}(D) - E_{red}(A)) - e^2/(4\pi\epsilon R_{DA}) + C$$

with $E_{ox}(D)$ and $E_{red}(A)$ being the oxidation potential of the donor and reduction potential of the acceptor group, respectively, in the chosen solvent. R_{DA} represents the distance across which the electron must be transferred. $C = T\Delta S$ compensates for entropy changes and was estimated to be on the order of 0.1 eV.[38c]

The oxidation and reduction potentials, which were determined for dyad 3 in THF ($\epsilon_r = 7.58$), are essentially equal to the oxidation potential of *N*-methylphenothiazine and the reduction potential of methylpyrene. The distance R_{DA} can be estimated either from the molecular structure by making reasonable assumptions on the center of gravity of the positive and negative excess charge or from the dipole moment derived from the Lippert−Mataga plot.

We assume the center of the positive charge to lie in the middle between the nitrogen and the sulfur atom of pheno-

TABLE 8: Parameters Derived from Lippert−Mataga Plots Based on Data Presented in Figures 4 and 5a, Respectively

	Figure 4 (7 data points)	Figure 4 (5 data points)	Figure 5a
$\tilde{\nu}$ vac/cm^{-1}	18870	24340	21725
slope/cm^{-1}	−22970	−24790	−20329
a^3/Å^3	194	194	194
μ_{CT}/D[a]	21	21.8	19.8

[a] Calculated with assumption $\mu_G = 0$.

thiazine and the center of the negative charge to be in the middle of the central (double) bond of pyrene. Then the distances R_{DA} are: for isomer 1 $R_{DA} = 5.78$ Å and for isomer 2 $R_{DA} = 5.89$ Å. The distances are reduced to 4.35 Å if the nitrogen lone pair is assumed to be the only donor function.

In the Lippert−Mataga plot (Figure 5b), the shift of the fluorescence maximum in a solvent with permittivity ϵ and refractive index n is approximated as[35]

$$\Delta\tilde{\nu}_F = \frac{1}{4\pi\epsilon_0 hc}\cdot\frac{2}{a^3}\cdot(\vec{\mu}_E - \vec{\mu}_G)\cdot\vec{\mu}_E\cdot f'(\epsilon,n)$$

where a represents the radius of the solvent cavity, $\vec{\mu}_G$ and $\vec{\mu}_E$ are the dipole moments in the ground and excited electronic states, respectively, and $f'(\epsilon,n)$ is the solvent polarity parameter

$$f'(\epsilon,n) = \frac{\epsilon - 1}{2\epsilon + 1} - \frac{1}{2}\frac{n^2 - 1}{2n^2 + 1}$$

To obtain an estimate of a^3, we determined the solvent-excluded volume for dyad 3 and calculated the radius of a sphere with the same volume. By employing this value, we can quantify the dipole moment of the CT state that produces the "red" fluorescence contribution. In a nonpolar solvent (MCH), the result is 21 D, and in polar solvents, it is 22 D (Table 8). Accordingly, the distances across which a unit charge must be transferred are 3.64 and 3.82 Å.

Finally, we can compute a distance, across which one unit charge must be transferred to yield the same dipole moment as calculated for the S_6 state (27 D). For the full CT state, the effective distance would be approximately the same in both isomers, namely, 5.78 Å.

By using the experimentally determined oxidation and reduction potentials of dyad 3, we can evaluate ΔG_{CT} in THF for the different estimates of R_{DA}. Depending on the adopted value of R_{DA}, the energy of the CT state lies between 2.45 and 2.53 eV above the electronic ground state. A comparison with the estimates for E_{00}(pyrene) = 3.3 eV and E_{00}(phenothiazine) = 3.03 eV implies that photoinduced electron transfer should indeed be a strongly exergonic process even in only solvents of medium polarity, quite in accord with the experimental finding.

There is another interesting aspect to the above estimate of the energy of the CT state. In a flash photolysis experiment, we found that the transient absorption spectrum of dyad 3, when measured in methylene chloride, exhibits the characteristic features of the pyrene triplet−triplet absorption.[39] However, in contrast to the measurements in cyclohexane, no indication for a population of the phenothiazine triplet was found. This finding suggests that in medium polar solvents the CT state of dyad 3 is higher in energy than the triplet state of pyrene (2.1 eV)[40] but lower than the triplet state of phenothiazine (2.62 eV).[41] The above estimate is in accord with this conclusion. It provides evidence that the CT state can decay into locally excited triplet states in less polar solvents.

4. Discussion

The fluorescence excitation spectra provide unique evidence that the species that emits the "red" fluorescence with the characteristics of a CT fluorescence possesses a UV/vis absorption spectrum that differs from that of the "blue" emitting species. The similarity of the absorption profiles suggests the two species to be isomers. The quantum-chemical model calculations actually find two stereoisomers, whose absorption spectra appear only slightly shifted against each other. The lowest excited state represents a local excitation of the phenothiazine moiety in both isomers. Geometry relaxation in this excited state leads to a nearly complete planarisation of the phenothiazine group with the effect that the relaxed first excited state of both isomers become essentially indistinguishable (Figure 8).

The full CT state, which can be described as one electron excitation between the phenothiazine localized HOMO and the pyrene localized LUMO + 1, exhibits its energetic minimum at about the same geometry as the phenothiazine localized S_1 state. This means that the same relaxation coordinate could be active for both states. The energy of the pyrene localized exited states are fairly insensitive to this relaxation process. On the other hand, if one optimizes the geometry of the pyrene-localized S_2 state, then one again obtains an approximately planar geometry for phenothiazine, but the angle of torsion of the single bond is only about 70°. This means that for this state the relaxation coordinate is different.

Because the energies of the locally excited states and that of the relaxed CT state(s) are very close to each other in the two isomers described, there is no good reason to assume that electron transfer is allowed in one isomer and forbidden in the other for energetic reasons. The distinction in the behavior of the two isomers must therefore be sought in the course of the potential hypersurface or, more precisely speaking, on the location and/or height of the barrier along the reaction coordinate-(s). The key should be the first excited state with a large CT character, which, in the CI approximation, is described as the HOMO → LUMO transition mixed with some local excitation of the phenothiazine group. Even in the "in vacuo" calculations, this state (S_5 in isomer 1 and S_4 in isomer 2) is energetically only slightly above the local excitations of pyrene ($\Delta E \sim 2800$ cm^{-1} or 0.35 eV) This implies that stabilization of this state by a polar solvent results in a near degeneracy of the CT and the pyrene LE state(s) and concomitantly in a strong mixing. The mixing pattern should be different in the two isomers and may result in different barriers for the transition from the LE state-(s) to either one of the CT states. Remember, that in the framework of simple transition state theory, a difference in barrier height of less than 6 kJ/mol is sufficient to explain a factor of 10 in reaction rate at ambient temperature assuming the same preexponential factor.

Inspection of Scheme 3 shows that indeed one finds a level crossing between the various locally excited states and the states with charge-transfer character.

The calculated barriers for electron transfer are different in the two isomers, as expected and confirm, in principle, the proposed model. Because the model calculations tend to overestimate the energy needed for charge separation, the real values of the barriers heights could be significantly lower.

A model that can explain the experimental findings must comprise the following assumptions:

(i) Energy transfer between pyrene and phenothiazine is inefficient (slow internal conversion $S_2 \rightarrow S_1$).

(ii) Electron transfer from either of the two locally excited states is fast in one of the two conformers. Fluorescence from the locally excited states is heavily quenched in this conformer.

(iii) In the second conformer, electron transfer is slowed because of a significantly higher barrier. Consequently, fluorescence from the locally excited states occurs, although with a reduced efficiency.

Energy transfer between excited pyrene and phenothiazine is of low efficiency only, despite the short distance due to the small Förster radius calculated on the ground of the experimental pyrene fluorescence and phenothiazine absorption spectra.[39] Moreover, there is no random distribution of the orientation of the transition dipole moments of donor and acceptor, which would allow us to use an orientation factor $\kappa^2 = 0.66$. Because of the actual short distance between donor and acceptor, a multipole expansion would be necessary to evaluate a proper κ^2 for the rather limited range of relative orientations of donor and acceptor.[40]

The proposed model can possibly also explain why the yield of CT fluorescence decreases with pressure although the decay time is invariant. Upon increase of the hydrostatic pressure, both the dielectric constant ϵ and the viscosity η of the solvent increase. The increase of the dielectric constant would lead to a decrease of the activation energy if the transition state exhibits a higher dipole moment than the starting state. Because the relative change of ϵ is small, this effect is probably not of great importance in our case. The increase of the viscosity of methylcyclohexane is very pronounced in the pressure range employed. Consequently, one could argue that the geometrical relaxation, which is the prerequisite for the formation of the relaxed charge transfer state, is strongly hampered by the increased solvent viscosity, and the yield of formation of the CT state is reduced. In addition, the rates for transition to the locally excited triplet states and the ground state are not changed significantly because of the small effect on the energy of the CT state. The behavior of dyad 3 contrasts with that of DMABN, where an increase of pressure favors the formation of the CT state because the effect of the increase of ϵ (stabilization of the CT state) overcompensates the retardation due to an increased viscosity.[43]

If we accept the possibility that in nonpolar solvents the lower lying of the two CT states (characterized as the HOMO $\rightarrow$ LUMO transition) becomes stabilized enough to allow an exergonic electron transfer from the pyrene excited state, then the results of the model calculations provide an explanation as to why in nonpolar solvents the dipole moment of the emitting CT state is smaller than that derived from the fluorescence in polar solvents.

In the latter solvents, the full CT state keeps its large dipole moment ($\sim$26.5 D). The first, lower-lying CT state exhibits an increased dipole moment because the mixing-in of configurations representing local excitations of phenothiazine is reduced. This increase of the dipole moment probably determines that the HOMO $\rightarrow$ LUMO based excited state stays the lowest state with charge-transfer character independent of solvent polarity.

If we accept the estimate that the relaxed CT state lies about 2.5 eV above the ground state, then excitation into the lowest excited state of the phenothiazine moiety should provide enough energy ($E_\infty = 2.97$ eV) for electron transfer from this state to represent an exergonic process in (medium) polar solvents. The difference between the estimated energy of the CT state and the observed radiative transition energy (fluorescence maximum) allows a rough estimate of the total reorganization energy in the electronic ground state

$$\lambda_{tot} = \Delta H_{CT} - h\nu_{CT} = 2.5 \text{ eV} - 2.15 \text{ eV}_{(THF)} \sim 0.35 \text{ eV}$$

This number compares well with the reorganization energy derived from the quantum chemical calculations.

5. Summary and Conclusion

We have provided strong evidence that the phenothiazine−pyrene electron donor−acceptor system investigated can exist in solution as two different conformers with dramatically different photophysical properties. This difference exists despite the great similarity of the properties of the excited states for the ground state optimized geometries and the geometries present in the fully relaxed charge transfer states.

Because energy transfer from excited pyrene to phenothiazine (internal conversion $S_2 \rightarrow S_1$) is small due to negligible overlap between pyrene fluorescence and phenothiazine absorption spectra, electron transfer can start from either excited state depending on excitation wavelength. In one isomer, electron transfer is obviously a barrierless process for both locally excited states occurring with a rate constant of $k_{et} \sim 10^{11}$ s^{-1}. In the other isomer, because of a modified CI description of the lowest charge transfer state, there exists a barrier along the reaction coordinate with the effect that the rate k_{et} is greatly reduced if either pyrene or phenothiazine is excited. This implies that the decay time of the phenothiazine type fluorescence emitted by isomer 2 is somewhat shorter compared to that of *N*-methylphenothiazine. The apparent shortening of the pyrene-type emission could be due to both energy transfer and to electron transfer, although with a greatly reduced efficiency.

The data presented show once again that consideration of geometrical relaxation is important for explaining the photophysical parameters of nonrigid systems.

Acknowledgment. The authors thank Prof. J. Daub (Universitaet Regensburg) for the donation of samples and many stimulating discussions. Financial support by Volkswagen-Stiftung, Deutsche Forschungsgemeinschaft and Fonds der Chemischen Industrie is gratefully acknowledged.

Supporting Information Available: One example of an experimental fluorescence decay curve with fit function and residuals (Figure S1), calculated geometries of the two isomers (Figure S2), schematic presentation of molecular orbitals of conformer 1 (Figure S3), molecular electrostatic potentials of the two different CT states of conformer 1 (Figure S4). This material is available free of charge via the Internet at http://pubs.acs.org.

References and Notes

(1) (a) Paddon-Row, M. N. *Acc. Chem. Res.* **1994**, *27*, 18. (b) Wasielewski, M. R. *Chem. Rev.* **1992**, *92*, 435. (c) Gust, D.; Moore, T. A.; Moore, A. L. *Acc. Chem. Res.* **1993**, *26*, 198.

(2) (a) Lauteslager, X. Y.; van Stokkum, I. H. M.; van Ramesdonk, H. J.; Bebelaar, D.; Fraanje, J.; Goubitz, K.; Schenk, H.; Brouwer, A. M.; Verhoeven, J. W. *Eur. J. Org. Chem.* **2001**, 3105. (b) Hviid, L.; Brouwer, A. M.; Paddon-Row, M. N.; Verhoeven, J. W. *Chem. Phys. Chem.* **2001**, *4*, 232.

(3) (a) Lukas, A. S.; Miller, S. E.; Wasielewski, M. R. *J. Phys. Chem. B* **2000**, *104*, 931. (b) Sinks, L. E.; Wasielewski, M. R. *J. Phys. Chem. A* **2003**, *107*, 611.

(4) Springer, J.; Kodis, G.; de la Garza, L.; Moore, A. L.; Moore, T. A.; Gust, D. *J. Phys. Chem. A* **2003**, *107*, 3567.

(5) Nelson, S. F. *Chem. Eur. J.* **2000**, *6*, 581.

(6) (a) Kurebayashi, H.; Fukazawa, Y. *Chem. Lett.* **2000**, 530. (b) Kurebayashi, H.; Sakaguchi, M.; Okajima, T.; Haino, T.; Usui, S.; Fukazawa, Y. *Tetrahedron Lett.* **1999**, *40*, 5545.

(7) (a) Zachariasse, K. A.; Grobys, M.; von der Haar, T.; Hebecker, A.; Il'ichev, Y. V.; Jiang, Y.-B.; Morawski, O.; Kuehnle, W. *J. Photochem. Photobiol. A* **1996**, *102*, 59. (b) Ma, C.; Kwok, W. M.; Matousek, P.; Parker, A. W.; Phillips, D.; Toner, W. T.; Towrie, M. *J. Phys. Chem. A* **2002**, *106*, 3294. (c) Rettig, W.; Lutze, S. *Chem. Phys. Lett.* **2001**, *341*, 263.

(8) (a) Read, I.; Napper, A. M.; Kaplan, R.; Zimmt, M. B.; Waldeck, D. H. *J. Am. Chem. Soc.* **1999**, *121*, 10976. (b) Napper, A. M.; Read, I.; Kaplan, R.; Zimmt, M. B.; Waldeck, D. H. *J. Phys. Chem. A* **2002**, *106*, 5288.

(9) Ramsteiner, I. B.; Hartschuh, A.; Port, H. *Chem. Phys. Lett.* **2001**, *343*, 83.

(10) Luo, C.; Guldi, D. M.; Imahori, H.; Tamaki, K.; Sakata, S. *J. Am. Chem. Soc.* **2000**, *122*, 6535.

(11) (a) Verhoeven, J. W.; Wegewijs, B.; Scherer, T.; Rettschnik, R. P. H.; Warman, J. M.; Jäger, W.; Schneider, S. *J. Phys. Org. Chem.* **1996**, *9*, 387. (b) Jäger, W.; Schneider, S.; Lauteslager, X. Y.; Verhoeven, J. W. *J. Phys. Chem.* **1996**, *100*, 8118. (c) Jäger, W.; Schneider, S.; Verhoeven, J. W. *Chem. Phys. Lett.* **1997**, *270*, 50. (d) Lauteslager, X. Y.; van Stokkum, I. H. M.; van Ramesdonk, H. J.; Brouwer, A. M.; Verhoeven, J. W. *J. Phys. Chem.* **1999**, *103*, 653.

(12) (a) Seischab, M.; Lodenkemper, Th.; Stockmann, A.; Schneider, S.; Koeberg, M.; Roest, M. R.; Verhoeven, J. W.; Lawson, J. M.; Paddon-Row, M. N. *Phys. Chem. Chem. Phys.* **2000**, *2*, 1889. (b) Goes, M.; de Groot, M.; Koeberg, M.; Verhoeven, J. W.; Lokan, N. R.; Shephard, M. J.; Paddon-Row, M. N. *J. Phys. Chem. A* **2002**, *106*, 2129.53. (c) Koeberg, M.; de Groot, M.; Verhoeven, J. W.; Lokan, N. R.; Shephard, M. J.; Paddon-Row, M. N. *J. Phys. Chem. A* **2001**, *105* (13), 3417. (d) Shephard, M. J.; Paddon-Row, M. N. *J. Phys. Chem. A* **2000**, *104* (49), 11628.

(13) (a) Bleisteiner, B.; Marian, T.; Schneider, S.; Brouwer, A. M.; Verhoeven, J. W. *Phys. Chem. Chem. Phys.* **2001**, *3*, 2070. (b) Bleisteiner, B.; Marian, T.; Schneider, S.; Brouwer, A. M.; Verhoeven, J. W. *Phys. Chem. Chem. Phys.* **2001**, *3*, 5392. (c) Bleisteiner, B.; Schneider, S.; Clark, T. *J. Mol. Model.* **2002**, *8*, 87. (d) Amini, A.; Harriman, A. *Phys. Chem. Chem. Phys.* **2003**, *5*, 1344. (e) Bell, T. D. M.; Joliffe, K. A.; Ghiggino, K. P.; Oliver, A. M.; Shephard, M. J.; Langford, S. J.; Paddon-Row, M. N. *J. Am. Chem. Soc.* **2000**, *122* (43), 10661.

(14) (a) Marcus, R. *J. Phys. Chem.* **1965**, *43*, 679. (b) Hush, N. S. *Chem. Phys. Lett.* **1988**, *143*, 488. (c) Brunschwig, B. S.; Ehrenson, S.; Sutin, N. *J. Chem. Phys.* **1987**, *91*, 4714.

(15) (a) Bodea, C.; Silberg, I. *Adv. Heterocyclic Chem.* **1968**, *9*, 321. (b) Gupta, R. R. *Phenothiazines and 1,4-Benzothiazines in Bioactive Molecules*; Elsevier: Amsterdam, 1988; p 4.

(16) (a) von der Haar, Th.; Hebecker, A.; Il'lchev, Y.; Kuehnle, W.; Zachariasse, K. A. *AIP Conf. Proc.* **1996**, *364*, 295. (b) Borowicz, P.; Herbich, J.; Kapturkiewicz, A.; Opallo, M.; Nowacki, J. *J. Chem. Phys.* **1999**, *249*, 49.

(17) Daub, J.; Engl, R.; Kurzawa, J.; Miller, S. E.; Schneider, S.; Stockmann A.; Wasielewski, M. R. *J. Phys. Chem. A* **2001**, *105*, 5655.

(18) (a) Stockmann, A.; Kurzawa, J.; Fritz, N.; Acar, N.; Schneider, S.; Daub, J.; Engl, R.; Clark, T. *J. Phys. Chem. A* **2002**, *106*, 7958. (b) Bleisteiner, B.; Marian, Th.; Schneider, S.; Brouwer, A. M.; Verhoeven, J. W. *Phys. Chem. Chem. Phys.* **2001**, *3*, 2070.

(19) Schneider, S.; Kurzawa, J.; Stockmann, A.; Engl, R.; Daub, J.; Matousek, P.; Towrie, M. *Chem. Phys. Lett.* **2001**, *348*, 277.

(20) Engl, R. Ph.D. Thesis, Universität Regensburg, Germany, 1999.

(21) Kemnitz, K.; Pfeifer, L.; Ainbund, M. *Nucl. Instr. Methods Phys. Res. A* **1997**, *387*, 86.

(22) (a) Stockmann, A. Ph.D. Thesis, Universität Erlangen-Nürnberg, Germany, 2001. (b) Jäger, W. Ph.D. Thesis, Universität Erlangen-Nürnberg, Germany, 1997.

(23) Gedeck, P.; Fluorescence decay fit program (Fld Fit) for IBM-compatible computers developed in the course of his Ph.D. Thesis, Universität Erlangen-Nürnberg, Germany, 1996.

(24) (a) Bevington, P. R.; Robinson, D. K. *Data Reduction and error analysis for the physical sciences*; The Mc-Graw Hill Companies, Inc.: Boston, 1992. (b) http://world.std.com/nr. *Numerical Recipies in C*; Cambridge University Press: Cambridge, 1992.

(25) Schneider, S.; Stockmann, A. *Opt. Express* **2000**, *6*, 220.

(26) Clark, T.; Alex, A.; Beck, B.; Burkhardt, F.; Chandrasekhar, J.; Gedeck, P.; Horn, A.; Hutter, M.; Martin, B.; Rauhut, G.; Sauer, W.; Schindler, T.; Steinke, T. *Vamp 8.0*; University of Erlangen: Erlangen, Germany, 2002.

(27) (a) Dewar, M. J. S.; Zoebisch, E.; Healy, E. F.; Stewart, J. J. P. *J. Am. Chem. Soc.* **1985**, *107*, 3902. (b) Holder, A. J. In *Encyclopedia of Computational Chemistry*; Schleyer, P. v. R., Allinger, N. L., Clark, T., Gasteiger, J., Kollman, P. A., Schaefer, H. F., III., Schreiner, P. R., Eds.; Wiley: Chichester, 1998; pp 1, 8.

(28) Clark, T.; Chandrasekhar, J. *Isr. J. Chem.* **1993**, *33*, 435.

(29) Dewar, M. J. S.; Liotard, D. A. *J. Mol. Struct. (THEOCHEM)* **1990**, *206*, 123.

(30) Rauhut, G.; Clark, T.; Steinke, T. *J. Am. Chem. Soc.* **1993**, *115*, 9174.

(31) Gedeck, P.; Schneider, S. *J. Photochem. Photobiol. A: Chem.* **1997**, *105*, 165.

(32) Rauhut, G.; Clark, T. *J. Comput. Chem.* **1993**, *14*, 503. Beck, B.; Rauhut, G.; Clark, T. *J. Comput. Chem.* **1994**, *15*, 1064.

(33) (a) Pascual-Ahuir, J. L.; Silla, E.; Tuñon, I. *J. Comput. Chem.* **1994**, *15*, 1127. (b) Marsili, M.; Floersheim, P.; Dreiding, A. S. *Comput. Chem.* **1993**, *7*, 175. (c) Lorensen, W.; Cline, H. *Comput. Graph.* **1987**, *21*, 163.

(34) Bondi, A. *J. Phys. Chem.* **1964**, *68*, 441.

(35) (a) Lippert, E. *Z. Elektrochem.* **1957**, *61*, 962. (b) Mataga, N.; Kaifu, Y.; Koizumi, M. *Bull. Chem. Soc. Jpn.* **1956**, *29*, 465.

(36) (a) Jonas, J.; Hasha, D.; Huang, S. G. *J. Chem. Phys.* **1979**, *1*, 887. (b) Brazier, D. W.; Freeman, G. R. *Can. J. Chem.* **1969**, *47*, 893.

(37) Kurzawa, J. Ph.D. Thesis, Universität Erlangen-Nürnberg, Germany, 2003.

(38) (a) Beens, H.; Weller, A. *Chem. Phys. Lett.* **1968**, 140. (b) Knibbe, H.; Rehm, D.; Weller, A. *Ber. Bunsen-Ges. Phys. Chem.* **1969**, *73*, 839. (c) Weller, A. *Z. Phys. Chem.* **1982**, *133*, 93. (a) Förster, Th. *Ann. Phys.* **1948**, *2*, 55.

(39) Bohne, C.; Abuin, E.; Sciano J. *J. Am. Chem. Soc.* **1990**, *112*, 4226.

(40) (a) Birks, J. *Photophysics of aromatic molecules*; John Wiley and Sons: New York, 1969. (b) Murov, S.; Carmichael, I.; Hug, G. *Handbook of Photochemistry*; Marcel Dekker Inc.: New York, 1993.

(41) Alkaitis, S.; Graettel, M.; Henglein, A. *Ber. Bunsen-Ges. Phys. Chem.* **1975**, *79*, 541.

(42) Förster, Th. *Fluoreszenz organischer Verbindungen*; Vandenhoeck & Rupprecht, Göttingen, Germany, 1951.

(43) Le Bret, M.; Le Pecq, J. B.; Barbet, J.; Roques, B. P. *Nucleic Acids Res.* **1977**, *4*, 1361.

(44) Grobys, M.; Zachariasse, K. A. *J. Inf. Recording* **1998**, *24*, 405.